Supporting Information for

Garnet Solid-State Electrolyte with Benzenedithiolate Catholyte for Rechargeable Lithium Battery

Bo Wang[a†], Yang Jin[b†], Yubing Si[a†], Wei Guo[a], and Yongzhu Fu[a,*]

1.1 Material

Li_2CO_3 (Sinopharm, 99.99%), La_2O_3 (Sinopharm, 99.99%, dried at 900 °C for 12 h), ZrO_2 (Aladdin, 99.99%), and Ta_2O_5 (Ourchem, 99.99%) powder was mixed together at a molar ratio of $Li_{6.4}La_3Zr_{1.4}Ta_{0.6}O_{12}$ (30% excess Li_2CO_3 was added) and ground with an agate mortar and pestle and then heated at 900 °C for 6 h to decompose the metal salts. The resulting powder was ball milled for 12 h, before being pressed into a pellet under 220 MPa cold isostatic pressing for 90 s, and then annealed at 1,140 °C for 16 h in air while the pellet was covered with the same mother powder. All heat treatments were conducted in alumina crucibles (>99% Al_2O_3) covered with alumina lids. The sintered $Li_{6.4}La_3Zr_{1.4}Ta_{0.6}O_{12}$ (LLZTO) pellet was sliced using a low speed diamond saw, and the thickness of the sliced LLZTO was ~700 μm.[1] The ionic conductivity of the prepared LLZTO is 3.21×10^{-4} S cm^{-2}.

1,2-benzenedithiol (1,2-BDT, >98%) was purchased and used as received. Appropriate amount of 1,2-BDT was added in Li-S electrolyte which consists of 1.0 M lithium bis(trifluoromethanesulphonyl)imide (LiTFSI) and 0.1 wt.% lithium nitrate ($LiNO_3$) in the mixture solvent of 1,2-dimethoxyethane (DME) and 1,3-dioxolane (DOL) (1:1 v/v) to render 0.10 and 0.15 M catholytes. Pieces of lithium metal were immersed in the catholytes to lithiate 1,2-BDT to form lithium 1,2-benzenedithiolate (1,2-LBDT). The catholytes were prepared and stored in an Argon filled glove box.

1.2 Battery assembly and electrochemical evaluation

In this study, commercial binder-free carbon nanotube paper called bucky paper (Nanotech Labs, Inc) was used as the current collector. The carbon paper was cut into 1.13 cm^2 discs (d = 12 mm, about 2 mg each) and dried at 100 °C for 24 h in a vacuum oven before use. Coin cells CR2032 were fabricated in the glove box. Firstly, 30 μL of catholyte was added into the bucky paper current collector. Then a Celgard 2400 or LLZTO was placed on the top of the electrode followed by adding 10 μL blank electrolyte on the top of the Celgard separator. Finally, lithium metal anode was placed on the separator. The cells were taken out of the glove box for testing.

Cyclic voltammetry (CV) was performed on a Bio-Logic SAS VMP-3 multichannel electrochemical workstation. The potential was swept from open circuit voltage to 3.0 V and then swept back to 1.8 V at a scanning rate of 0.05 mV s^{-1}. Cells were galvanostatically cycled between 1.8 and 3 V on an LANHE CT2001A battery test system at different C rates (1 C = 347.6 mA g^{-1}). The electrochemical impedance spectroscopy (EIS) was measured by an

electrochemical workstation (CHI761E) in the frequency range from 10^5 Hz to 1 Hz with a perturbation of 5 mV. All the tests were conducted at ambient temperature.

1.3 Characterization

After 100 cycles, the LLZTO cell was dissembled and the LLZTO pellet was characterized by X-ray diffraction (XRD) on a Rigaku MiniFlex 600 XRD Instrument equipped with Cu Kα radiation. Powder XRD was employed to monitor the phase formation in the 2θ range from 10 to 70° with a step size of 0.02°. To avoid exposure of the LLZTO electrolyte to air, the samples were protected with Kapton film in the sample holder during the measurements. The morphological characterization of the discharged electrodes was conducted with a Carl Zeiss Sigma 500 field emission scanning electron microscopy (SEM). To minimize the exposure of the samples to air, they were prepared in glove box and transferred to the SEM chamber in an Argon-filled bag. X-ray photoelectron spectroscopy (XPS) measurements were conducted with PHI 5000 VersaProbe II.

1.4 Computational details

In this work, the structure of LLZTO was prepared by Special Quasirandom Structure (SQS) method in the Alloy Theoretic Automated Toolkit (ATAT).[2-4] All the calculations were performed based on density function theory (DFT) within generalized gradient approximation in the Perde-Burke-Ernzerh (PBE) scheme, as implemented in the Vienna ab initio simulation package (VASP) code.[5-7] The valence electronic states were expanded in plane wave basis sets with an energy cutoff of 400 eV. The energy optimization was considered completed with force convergence criterion of 10 meV $Å^{-1}$. We used the Monkhorst-Pack k-point mesh of 3×3×1 for surface structural relaxation and a vacuum slab of about 15 Å was employed. The LLZTO (100) surface was chosen to calculate the adsorption energies. The adsorption energies (E_a) for the charge product (Ph_2S_4) and discharge product ($PhLi_2S_2$) on the metal oxide surfaces are defined as $E_a=E_{total}–E_{com}–E_{suf}$, where E_{total} is the total energy of the adsorbed system, E_{com} is the energy of the compound in vacuum, and E_{suf} is the energy of the optimized clean surface slab.

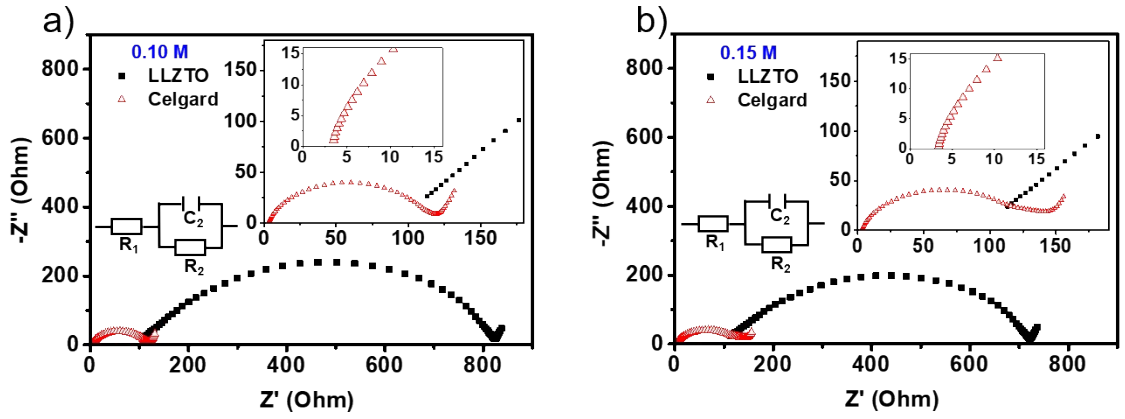

Figure S1. The resistance of the LBDT and LBDT-LLZTO cell. R_1 is bulk resistance of the electrolyte; R_2 is the interfacial resistance.

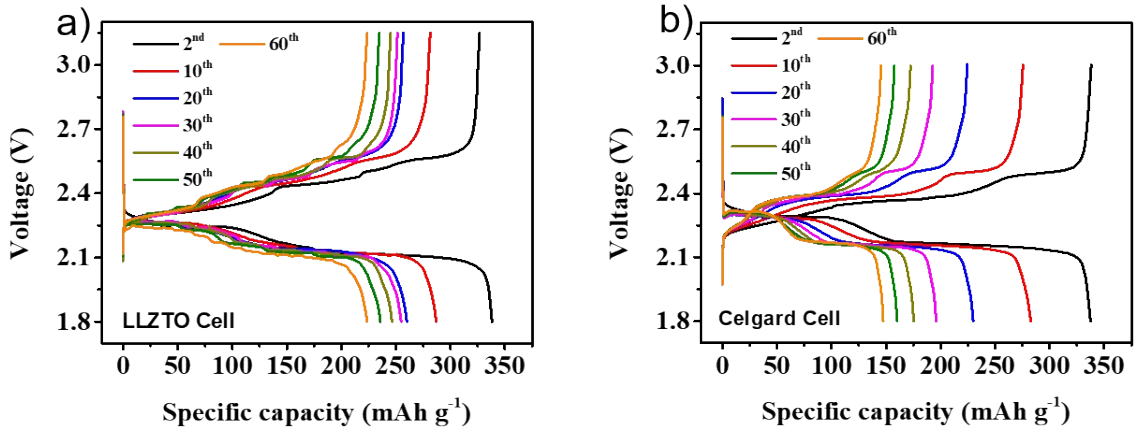

Figure S2. Voltage profile of the LLZTO cell and the Celgard cell at different cycle, the concertation of the catholyte is 0.15 M.

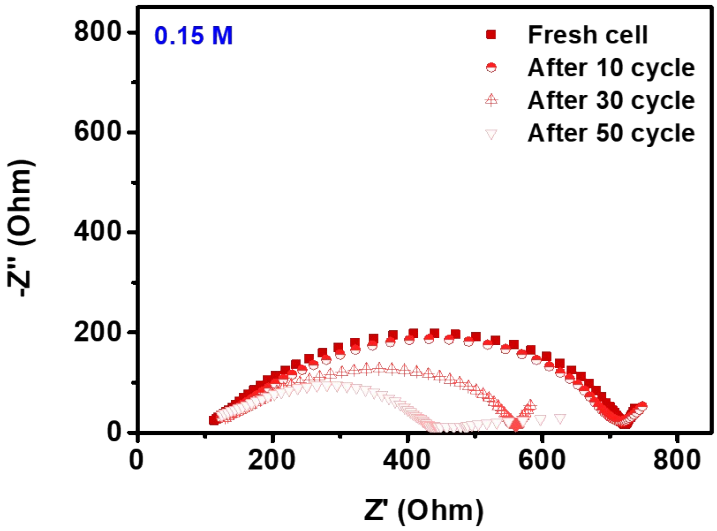

Figure S3. Nyquist plots of the LLZTO cell after different cycles, the concertation of the catholyte is 0.15 M.

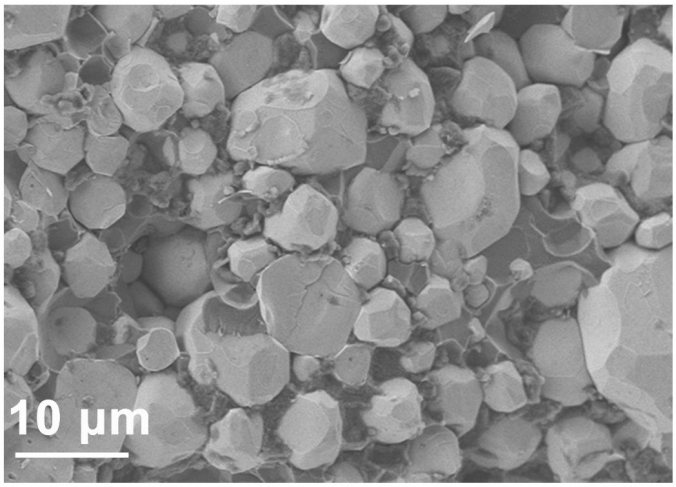

Figure S4. SEM of the fresh LLZTO.

Table S1. Binding energies of the different elements and their values.

Element	Band	Binding Energy /eV	References
C	$-CF_3$ LiTFSI	291.3	8
	-C-O Li_2CO_3	290.5	9, 10
	O-C-O DOL/DME	287.0	11
La	La-O	102.0	12
S	-S-O LiTFSI	169.8, 167.8	10, 13
	-S-S- Ph_2S_4	164.8, 166.9	10, 13
	-S-Li $Ph_2S_2Li_2$	161.6, 163.2	10, 13
O	-C-O Li_2CO_3	532.3	8
	-S-O LiTFSI	533.3	14, 15
	-O-Li- LLZTO-LiSPh	531.5	
	O-M LLZTO	529.4	14, 15

References:

1. Y. Jin, K. Liu, J. Lang, D. Zhuo, Z. Huang, C.-a. Wang, H. Wu and Y. Cui, *Nat. Energy*, 2018, **3**, 732.
2. A. van de Walle, *CALPHAD*, 2009, **33**, 266.
3. A. van de Walle, M. Asta and G. Ceder, *CALPHAD*, 2002, **26**, 539.
4. A. van de Walle and G. Ceder, *J. Phase Equilib.*, 2002, **23**, 348.
5. A. Scholze, W. G. Schmidt and F. Bechstedt, *Phys. Rev. B*, 1996, **53**, 13725.
6. G. Kresse and J. Furthmuller, *Comp. Mater. Sci.*, 1996, **6**, 15.
7. J. P. Perdew, K. Burke and M. Ernzerhof, *Phys. Rev. Lett.*, 1996, **77**, 3865.
8. S. Leroy, H. Martinez, R. Dedryvère, D. Lemordant and D. Gonbeau, *Appl. Surf. Sci.*, 2007, **253**, 4895.
9. F. Han, J. Yue, C. Chen, N. Zhao, X. Fan, Z. Ma, T. Gao, F. Wang, X. Guo and C. Wang, *Joule*, 2018, **2**, 497.
10. Y. Diao, K. Xie, S. Xiong and X. Hong, *J. Electrochem. Soc.*, 2012, **159**, A1816.
11. A. Sharafi, E. Kazyak, A. L. Davis, S. Yu, T. Thompson, D. J. Siegel, N. P. Dasgupta and J. Sakamoto, *Chem. Mater.*, 2017, **29**, 7961.
12. X. Zhan, S. Lai, M. P. Gobet, S. G. Greenbaum and M. Shirpour, *Phys. Chem. Chem. Phys.*, 2018, **20**, 1447.
13. Y. X. Wang, L. Huang, L. C. Sun, S. Y. Xie, G. L. Xu, S. R. Chen, Y. F. Xu, J. T. Li, S. L. Chou, S. X. Dou and S. G. Sun, *J. Mater. Chem.*, 2012, **22**, 4744.
14. A. Sharafi, S. Yu, M. Naguib, M. Lee, C. Ma, H. M. Meyer, J. Nanda, M. Chi, D. J. Siegel and J. Sakamoto, *J. Mater. Chem. A*, 2017, **5**, 13475.
15. Y. Zhu, J. G. Connell, S. Tepavcevic, P. Zapol, R. Garcia-Mendez, N. J. Taylor, J. Sakamoto, B. J. Ingram, L. A. Curtiss, J. W. Freeland, D. D. Fong and N. M. Markovic, *Adv. Energy Mater.*, 2019, **9**, 1803440.